

# A PRECISE MODEL FOR INTERVERTEBRAL DISC LOCALIZATION AND SEGMENTATION IN MRI USING A NOVEL LU-WOA-U NET ALGORITHM

**SPURTHI ADIBATTI**

Research Scholar, Department of ECE, BMSCE Bangalore.

**K.R SUDHINDRA**

Associate Professor, Department of ECE, BMSCE Bangalore.

**JOSHI MANISHA S**

Professor, Department of Medical Electronics, BMSCE Bangalore.

## Abstract

In the modern era, the advance technologies are entirely change the human lifestyle, behaviors and also, it is routine for daily life. For this reason, numerous diseases have been developed and cause death form illions of people every year. Although the degenerative process of the Intervertebral Disc (IVD) is not a deadly disease, this condition can't be cured instantaneously. Therefore, to address this issue a novel U-Net based Whale Optimization Algorithm (WOA) is developed. It is one of the Machine Learning (ML) algorithms for enhancing the efficiency of the segmentation process. Moreover, MRI images are used as the dataset of proposed model. To improve the classification process the collected MRI datasets are split into multiple segments. Consequently, the proposed technique includes three main phases such as 1.DataPre-processing2. Localization and finally, 3.Segmentation. Here, redundant noise and unwanted information of the input images are neglected with the help of Gaussian filtering function. Hereafter, preprocessed images are taken as localized images, and then localized images are segmented through theU- Net segmentation model which is designed with the efficiency of Lagrangian Updated-WOA(LU-WOA). Moreover, the performance of the proposed LU-WOA-UNet model is validated through a comparative analysis over state-of- the-art models interms of accuracy, sensitivity, specificity, and DSC.Besides, the proposed model achieved significant performances over the conventional models like DCNN, SVM, NN, FCN and SOTA.

**Keywords:** LU-WOA, UNet, Segmentation Localization, GLCM, Multi- ModalMRI.

## 1 Introduction

Recently, technology occupies the major routine of everyday human life which paves the way for more sedentary lifestyle habits [12]. A sedentary lifestyle is a major cause of many spine diseases lately. Medical experts stated that LBP is the most common spine disease and about 25% to 50% of adults are affected which causes disabilities and severely affecting the well-being of people [9][11]. Besides, in America, the medical expense for spine disease alone drastically increasing per year [28]. Even though LBP, Degenerative Disc Disease (DDD), and scoliosis can be last for years or lifelong, these diseases can be treated and cured with proper medication and treatment. For this reason, localization and segmentation of IVD are necessary to treat people [15][19]. Most specifically, early detection and appropriate treatment at right time can help to 90% successful cure [17]. However, localizing IVD at an early stage is a challenging one as it needs medical experts or experienced professionals for diagnosis [10].

With the Help of Artificial Intelligence (AI), and Computer-Aided Design (CAD) helps to reduce manual burden [13]. A lot of researches have been performed and proposed to develop effective IVD localization and segmentation methodologies to solve the issues and to help the IVD affected patients [16]. Previously, several ML algorithms were introduced for IVD localization and segmentation. There were several challenges that limits the accuracy performance. One of the major challenges is screening as well as handling ambiguous IVD boundaries [15][21]. Moreover, the controversies in accuracy restrict the complete automation of IVD localization and segmentation in the medical field. Later, ML algorithms provide better results in localizing and segmenting IVDs using MRI. Several ML algorithms are previously developed such as Support Vector Machine (SVM), K-Nearest Neighbor (KNN), Convolutional Neural Networks (CNN), Deep Belief Networks (DBN), Neural Networks (NN), U-NET, etc., helps detecting PCa [24][27][29][31]. Moreover, the SVM framework is performed in three stages, which are highlighting the structure of vertebrae boundaries, identify the vertebrae boundaries and observe the shapes. The KNN model is classify the hybrid feature and extract the affted parts from the collected datasets efficiently. After that, CNN modules it is most familiar model for all medical problems here, CNN is takes 359 images for training process. DBN model is efficiently enhancing the neurological condition detection and treatment procedures. In addition, the DBN is incorporated with optimization model to get better detection and segmentation accuracy. Also, it can recognize the spinal cord injury in an efficient way. Yet, the computational complexities in traditional algorithms limit efficiency. Accurate classification of benign or malignant MRI is a complex task [22]. Attaining new accuracy achievement is another complicated task in ML-based algorithms. Furthermore, the main concentration of the research involves detecting indolent displacements and severe fragmentation. Another major issue in ML algorithm is improper inputs leads to imprecise outputs [23][25]. Thus, creating a proper dataset is mandatory in image classification.

Intending to improve the accuracy performance, MRI has been implemented in localizing and segmenting IVDs [30]. Herein, an ensemble model of learning and training the algorithms have been greatly implemented and validate the extreme performance in several challenging image processing scenarios [14][26]. However, implementing ML approaches in IVD localization and segmentation requires more study and investigation so as to attain promising results [18]. Segmenting an image plays a crucial role in image processing as it helps to improvise classification performance. In previous researches, numerous image segmentation approaches have been developed [19][20]. Yet, the complexities and insignificant performance necessitate scholars to innovate more efficient techniques. Thereby, this paper aims to establish a novel methodology for localizing and segmenting IVDs using MRI data through the efficiency of ML algorithms and significant image segmentation techniques.

Algorithm of the proposed LU-WOA-UNet model is summarized as, initial process is update all the dataset to the input layer of the U-Net module and trained to the system. Then, the collected datasets are preprocessed and localized. Here, preprocessing side Gaussian function used and localization phase edge detection function is used.

Hereafter, based on the fitness function segmentation is performed and finally, suitable parameters are evaluated and that are illustrated in graphical representation.

The rest of the paper is organized as given as follows. Section II deals with the literature regarding previous and recent researches in IVD localization and segmentation. Section III presents the basic operations of the IVD localization and segmentation model and Section IV deals with the conventional and proposed WOA model. Besides, the experimental analysis and the attained results are demonstrated in Section V. and, Section VI concludes the paper.

## 2 Related works

In 2021, Das P et al. [1] Developed a model for identifying and segmenting IVDs using multi-modality MRI. Here a modified Deep NN (DNN) named Region-to-Image Matching Network (RIMNet) was used. Moreover, automatic and instantaneous detection and segmentation were implemented. From the investigation study, it attained better accuracy, Jaccard Coefficient, and F1-Score

In 2018, Kim S et al. [2] Addressed a model using an improved U-net for IVD segmentation. The limitations in traditional U-net such as complexities in the max-pooling layer were eliminated by employing a cascaded learning process to overwhelm the structural boundaries. The efficiency of the improved U-Net method was verified with a comparative analysis over the traditional U-Net and accomplished better Dice Similarity Coefficient (DSC).

**Table. 1 Research gap**

Method Name	Process	Features	Challenges
The RIMNet Method	IVD Identification and Segmentation	<ul style="list-style-type: none"> <li>An automated and simultaneous performance was achieved</li> <li>Attained considerable accuracy</li> </ul>	<ul style="list-style-type: none"> <li>Exposed complex architecture</li> <li>Revealed poor DSC</li> </ul>
The U-Net segmentation Method	IVD Segmentation	<ul style="list-style-type: none"> <li>Achieved considerable performance under weakly supervised conditions</li> <li>Accomplished minimized loss</li> </ul>	<ul style="list-style-type: none"> <li>Implemented using a small dataset</li> <li>Revealed poor performance under large testing data</li> </ul>
The Wavelet Decomposition and ICA-AAM Methods	IVD Segmentation and Classification	<ul style="list-style-type: none"> <li>Accomplished better accuracy</li> <li>Attained better segmentation results and stability</li> </ul>	<ul style="list-style-type: none"> <li>Exhibited complex expressions for multimodal registration of the features</li> </ul>

			<ul style="list-style-type: none"> <li>• Required high computational time</li> </ul>
The NN Method	IVD Segmentation	<ul style="list-style-type: none"> <li>• Obtained improved efficiency</li> <li>• Used multiple datasets to train the classifier</li> </ul>	<ul style="list-style-type: none"> <li>• Required high computation time for system initialization</li> <li>• Required manual assistance for ROI diagnosis</li> </ul>
The FCN Method	IVD Localization and Segmentation	<ul style="list-style-type: none"> <li>• Provided better performance with low-resolution MRI</li> <li>• Achieved better accuracy</li> </ul>	<ul style="list-style-type: none"> <li>• Leveraging the orthogonal background was complex</li> <li>• Implemented using a small amount of data</li> </ul>
The CNN Method	IVD Localization and Segmentation	<ul style="list-style-type: none"> <li>• Ensured better accuracy</li> <li>• Provided clear results for segmentation</li> </ul>	<ul style="list-style-type: none"> <li>• Attained imprecise performance</li> <li>• Implemented with a small amount of data</li> </ul>
The Median Filtering and Gradient Descent Methods	IVD Assessment	<ul style="list-style-type: none"> <li>• Bland-Altman plot was used to assess the IVDs</li> <li>• A novel IBD T2 was implemented</li> </ul>	<ul style="list-style-type: none"> <li>• It exhibited complicated assessment procedures</li> <li>• Data partition was complex</li> </ul>
The BPNN, KNN, and SVM Methods	IVD Classification	<ul style="list-style-type: none"> <li>• The efficiency of the ensemble model was analyzed</li> <li>• Attained better accuracy</li> </ul>	<ul style="list-style-type: none"> <li>• Computationally complex</li> <li>• Exhibited inconsiderable performance under 70% of training data</li> </ul>

In 2019, Yang Y et al. [3] established a novel wavelet image denoising and Independent Component Analysis-Active appearance Model (ICA-AAM) to segment and classify IVDs. Initially, the MRI data was decomposed and the noise was eliminated through wavelet transform and soft threshold approaches respectively. Further, segmentation was applied using AAM, and eventually, classification was performed. The ICA-AAM approach effectively locates and segments the IBDs and accomplished considerable accuracy.

In 2021, Abhinav Suri et al. [4] developed a DL scheme for IVD segmentation using MRI, Computed Tomography (CT), and X-ray images. Hither, a NN was implemented by provided training with 4490 MR, 550 CT, and 1935 X-ray images to attain 2D segmentation results. Through a 5-fold cross-validation approach, the NN

model achieved enhanced DSE and accuracy. Besides, this NN model exposed a faster computation.

In 2018, Li X et al. [5] introduced a Fully Convolutional Network (FCN) method for localization and segmentation of IVDs. In addition, four-modality MR data were implemented for better performance. Initially, the MR data was processed with several scales and combined only the significant features. Further, an arbitrary modality voxel dropout approach was performed to complement the harness.

In 2018, Wimmer Metal. [6] presented a novel spine labeling scheme using CNN from T1- and T2- weighted MR images, MR Dixon images, and CT images. Now, the localization and segmentation of IVDs were performed by merging the local entropy-optimized texture features and localize the sacral area. Besides, an intensity-based template-matching technique was applied to refine the data. From the experimental evaluation, the CNN model attained remarkable sacrum detection rate and sacrum localization accuracy.

In 2021, Belavy DLet al. [7] addressed an IVD assessment model to obtain reliable results using median filtering and gradient descent approaches. In this work, IVD T2 data has been used to assess the IVDs in consideration with the accomplishment of reliability. Moreover, the IVD T2 data was evaluated 9 times with a proper interval through a spin-echo multi-echo sequence and the repeatability was analyzed with Intra-class Correlation Coefficients (ICCs) was utilized. Through the Bland-Altman plot, the assessment for IVDs was checked in terms of reliability and repeatability.

In 2020, Hashia, B., and Mir, A.H [8] developed a DL approach by implementing an ensemble model through Back Propagation NN (BPNN), KNN, and SVM for IVD classification. Here, the significant features were extracted using three various approaches. Among them, Grey Level Run Length Matrix (GLRLM) technique extracted efficient Region of Interest (ROI). Furthermore, the SVM model attained enhanced accuracy among all the models.

Table I delivers the features and challenges associated with the IVD detection, localization, segmentation, and classification approaches using various ML models. Here, most of the implementations were performed using DL algorithms, and enhancements were applied to the training phase of the classifiers. Moreover, multi-modal MRIs were widely used for better performance.

The key contributions of the paper are stated below.

- Initially, IVD MRI datasets are collected from net source and it is taken as input images.
- Then, the collected datasets are trained to the system.
- After that, a novel optimized U-Net with LU-WOA replica is developed for entire phases.
- After that, the noises in the input images are eliminated through a data pre-processing phase using the Gaussian filtering technique.

- After the preprocessing, the significant features in the images are subjected to localization, and the localized images are given to the ML model for segmentation.
- Based on the WO fitness function the collected MRI images are segmented with suitable parameter.
- Then the performance of the proposed model is compared with other existing and the efficiency was verified in terms of, accuracy, sensitivity, specificity.

### 3. Proposed Architecture

In this subsection, the proposed architecture of IVD localization and segmentation is discussed. Fig. 1 is the depiction of the proposed model using ML algorithms. Here, 3D multi-modal MRI data have been utilized for image processing. At first, the MRI data are taken as input images for IVD localization. Intending to improve the performance, the noises in the input images are eliminated through a data pre-processing phase using the Gaussian filtering technique. The Basic Operations in Proposed Localization and Segmentation Model is illustrated in fig.1.

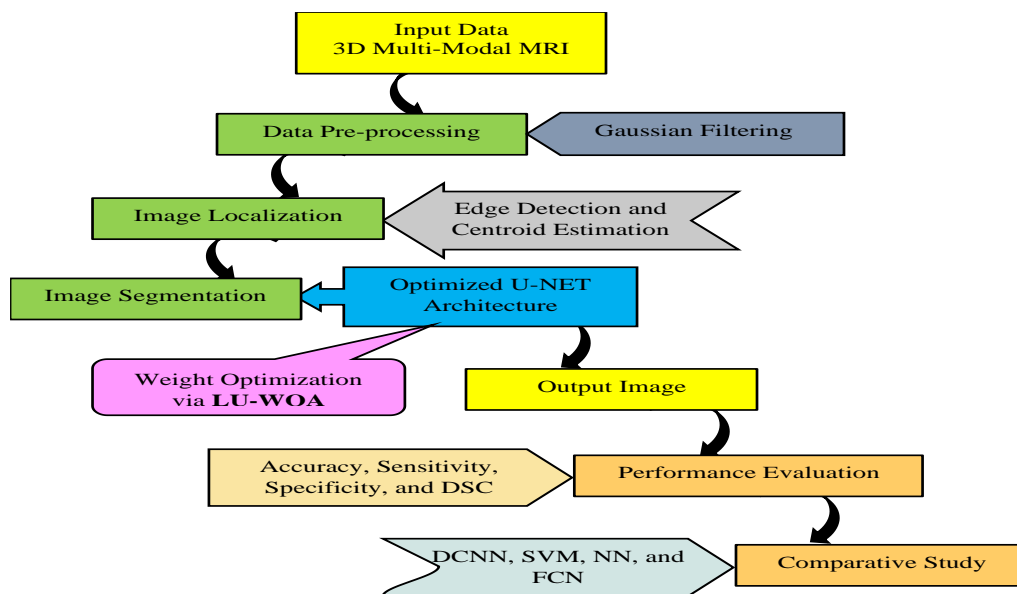


**Fig.1 Block Diagram of Proposed IVD localization and Segmentation Model**

Once removing the unnecessary data in the input images, the pre-processed images are subjected to localization, and the localized data are given as input to the U-Net segmentation process. In order to enhance the performance of the U-Net model, the efficacy of LU-WOA is employed to design the U-Net convolution layers.

#### 3.1 Data Preprocessing

The input image  $I_{input}$  can have noises or unnecessary distortions which are eliminated at this initial stage. Now, the  $I_{input}$  have four various image modalities such as in-phase  $I_{i1}$ , out-phase  $I_{i2}$ , fat  $I_{i3}$ , and water  $I_{i4}$  and all such images are needed to be improved. For this enhancement, the Gaussian filtering [34] approach is employed.

Generally, Gaussian filters impulse response using Gaussian function, and the mathematical model is given as follows. The 1D Gaussian filter and its impulse response and frequency response are stated in Eq. (1) and (2) respectively, in which  $\alpha$  indicates the function for Standard Deviation (SD)  $\sigma$ , and  $F$  specifies the frequency

$$G(a) = \sqrt{\frac{\alpha}{\pi}} e^{-\alpha a^2} \quad (1)$$

$$G(F) = e^{-\frac{\pi^2 F^2}{\alpha}} \quad (2)$$

Moreover, the standard deviation of Eq. (1) and (2) are given in Eq. (3) and (4).

$$G(a) = \frac{1}{\sqrt{2\pi\sigma}} e^{-\frac{\alpha a^2}{2\sigma^2}} \quad (3)$$

$$G(F) = e^{-\frac{F^2}{2\sigma_F^2}} \quad (4)$$

The 2D Gaussian function is applied as a multiplication of the above-mentioned Gaussians as stated in Eq. (5), in which  $a$  indicates horizontal axis and  $b$  denotes vertical axis. In this phase, the 3D input images are converted into 2D slices and further subjected for feature localization.

$$G_{out}(a, b) = \frac{1}{2\pi\sigma^2} e^{-\frac{a^2+b^2}{2\sigma^2}} \quad (5)$$

The main aim of this preprocess phase is to enhance the image quality, and then only easily use the next phases. Here, redundant information, undesired distortions and noises present in the collected input images are removed with help of suitable functions and operations.

### 3.2 Image Localization

The filtered image  $G_{out}$  is now given to the localization process. At this point, the localization is carried out based on locating the spines with respect to scale  $S$  and the directions  $D$ . The directions include vertical and horizontal planes and also, the spine structure is similar to a vertical direction. Thereby, the spine is localized by subtracting the mean of horizontal direction from vertical data.

$$L_s = \sum_{x \in X, y \in Y_1} L_{x,y} - \sum_{x \in X, y \in Y_2} L_{x,y} \quad (13)$$

Herein,  $x \in X = [0, 1, \dots, S - 1]$ , and  $y \in Y = [0, 1, \dots, D - 1]$ ,  $Y_1 = [0, 1, 2, 3, 4, 5, 11, 15]$ , and  $Y_2 = [7, 8, 9, 10, 11]$  indicates the directions closer to the spine. The edge points of the spines are represented by positive values are estimated using Eq. (14).

$$L_s(x, y) = \begin{cases} L_s(x, y) & L_s(x, y) \geq 0 \\ 0 & L_s(x, y) < 0 \end{cases} \quad (14)$$

With respect to the anatomical study, the angle of IVDs among the horizontal planes, as well as the longest axis is approximately  $\pm 30^\circ$ . Hence,  $Y_1 = [7, 8, 9, 10, 11]$  denotes the  $D$  near to the long axis and  $Y_2 = [1, 2, 3, 4, 5]$  points out the  $D$  near to vertical plane. Now, the centroid of the IVDs according to row values is estimated based on Eq. (15), in which  $L_r(n)$  portrays the centroid for first  $n$  columns,  $G$  points out the total count of rows of the image, and  $N$  is the number of columns.

$$L_r(n) = \sum_{x=1}^N L_m(x, n), \quad n = 1, \dots, G \quad (15)$$

Similarly, for column values, the centroid is calculated as per Eq. (16).

$$L_c(n) = \sum_{y=1}^G L_m(y, n), \quad n = 1, \dots, N \quad (16)$$

At last,  $(L_r(n), L_c(n))$  is the localized image given to U-Net segmentation.

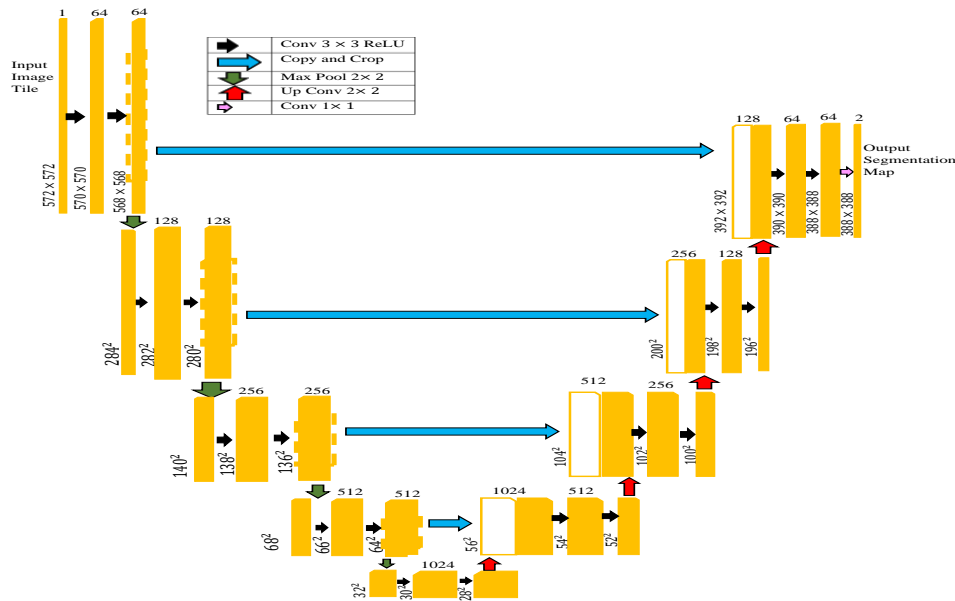


**Fig.2 Basic Architecture of U-Net for  $32 \times 32$  Pixel Resolution**

In the localization phase, recognize the exact location of more collected images and also identify the boundaries. Here, the proposed algorithm is to predict the image classes with discrete numbers. Moreover, the output is labeled with x, y coordinates.

### 3.3 Image Segmentation using U-NET

In this subsection, the proposed architecture of IVD segmentation is presented. Hither,  $(L_r(n), L_c(n))$  is given as input for U-Net segmentation. In general, U-Net [32] is modified versions of fully CNN which can perform efficiently even with limited datasets. The U-Net is constructed with an encoder-decoder configuration, in which the encoder is responsible for input features and considers only the significant features, whereas the decoder is responsible for learning the features from the encoder and provides better results for the actual input or desired outcome. The contracting and expansive path are two major sections in U-Net located on the left and right side and compute down-sampling and up-sampling respectively. Fig. 2 portrays the basic architecture of U-Net for  $32 \times 32$  pixel resolution. Now, the conventional U-Net architecture is optimized using LU-WOA.

## 4 Conventional and Proposed Optimization Concepts

### 4.1 Conventional WOA

Hither, the mathematical model of traditional WOA[33] is presented. In general, it exhibits the hunting behavior of Humpback whales and includes three basic steps such as encircling prey, spiralbubble-net feeding, and prey search. At first, the optimal

solution is unknown and the current solution is considered to be the best solution. Once the best solution is identified then the other solutions try to update their locations as per the best solution as stated in Eq. (17) and (18).

$$\hat{R} = |\hat{Q} \cdot \hat{A}_1(\tau) - \hat{A}(\tau)| \quad (17)$$

$$\hat{A}(\tau + 1) = \hat{A}_1(\tau) - \hat{B} \cdot \hat{R} \quad (18)$$

Now,  $\tau$  points to the present iteration,  $\hat{B}$  and  $\hat{Q}$  specifies the coefficient vectors,  $\hat{A}_1$  means to the location of an optimal solution, and  $\hat{A}$  defines the location vector. Besides, the notation  $| \cdot |$  represents absolute value and element-by-element multiplication. Eq. (19) and (20) portrays the evaluation of vectors  $\hat{B}$  and  $\hat{Q}$  in which,  $\hat{z}$  means to linearly minimized values in the range of 2 to 0 during the iterations and  $\hat{v}$  states arbitrary numbers from (0 – 1).

$$\hat{B} = 2\hat{z} \cdot \hat{v} - \hat{z} \quad (19)$$

$$\hat{Q} = 2 \cdot \hat{v} \quad (20)$$

In the spiral bubble-net attacking stage, the exploitation process is carried out through two sub-stages that is shrinking encircling strategy which is performed by minimizing the  $\hat{B}$  to  $\hat{z}$  in Eq. (19) and spiral location update is applied to determine the distance between whale and prey as stated in Eq. (21), in which  $u$  indicates a constant,  $k$  refers to an arbitrary number between  $[-1,1]$  and the notation  $\cdot$  points out element-by-element multiplication. Besides,  $\hat{R}' = |\hat{A}_1(\tau) - \hat{A}(\tau)|$  this denotes the distance between the whale and the prey.

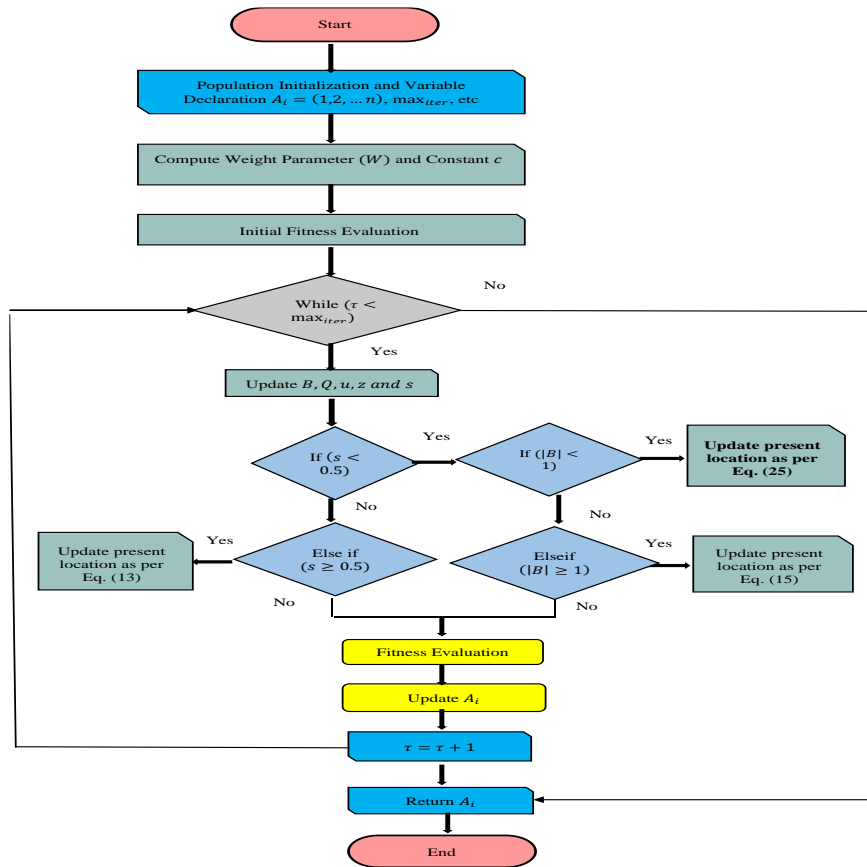


**Fig.3 Flow chart of Proposed Image Segmentation Model using ML Algorithms**

$$\hat{A}(\tau + 1) = \hat{R}' \cdot e_{uk} \cdot \cos(2\pi k) + \hat{A}_1(\tau) \quad (21)$$

Through the spiral bubble-net attacking approach, the solution update process is evaluated as given in Eq. (22), in which  $s$  is an arbitrary number between  $[0,1]$ .

$$\hat{A}(\tau + 1) = \begin{cases} \hat{A}_1(\tau) - \hat{B} \cdot \hat{R} & \text{if } s < 0.5 \\ \hat{R}' \cdot e_{uk} \cdot \cos(2\pi k) + \hat{A}_1(\tau) & \text{if } s \geq 0.5 \end{cases} \quad (22)$$

Subsequently, the search for prey that is the global search process in WOA is modeled as portrayed in Eq. (23) and (24). Table III illustrates the Algorithm of the WOA model.

$$\hat{R} = |\hat{Q} \cdot \hat{A}_{rand} - \hat{A}| \quad (23)$$

$$\hat{A}(\tau + 1) = \hat{A}_{rand} - \hat{B} \cdot \hat{Q} \quad (24)$$

#### 4.2 Proposed LU- WOA

As we know, WOA is efficient in handling complex optimization problems and requires a minimum count of pre-defined parameters. Besides, it is easy to implement and exhibits the proficiency of eliminating local optimum and attains global optimal solutions. Yet, it revealed poor computational speed in solving exponential complex problems. In addition, with regards to accurate performance, WOA fails to accomplish efficiently. At this point, the major intention of this paper is to achieve better accuracy

for IVD localization and segmentation using multi-modal MRI. Thereby, this paper introduces an improved WOA by replacing the conventional update expression given in Eq. (17) into a new one defined in Eq. (25), where  $\dot{w}(\tau)$  portrays the time derivative of  $w(\tau)$ .

$$\hat{R}(w) = \int_x^y L(\tau, w(\tau), \dot{w}(\tau)) d\tau \quad (25)$$

Here,  $(L, A)$  is the set of population space and Lagrangian  $L = L(\tau, w, v)$ ,  $w \in A$ , consider  $P(x, y, a_x, a_y)$  as the set of parameters from  $w: [x, y] \rightarrow A$ , where  $w(x) = a_x$  and  $w(y) = a_y$ . Now, the action function of  $L$  is given in Eq. (26), which is attained by solving Eq. (25).

$$\hat{R}: P(x, y, a_x, a_y) \rightarrow A \quad (26)$$

**Algorithm 1** shows the proposed LU-WOA model. Fig, 3 demonstrates the flowchart of the proposed LU-WOA model.

---

#### Algorithm 1: Proposed LU-WOA Model

---

**Input:** MRI images

**Start**

```

Initialize the population           // dataset initialization at input layer
{
    int  $A_i = (1, 2, \dots, n)$ 
}
Compute fitness function
    For each search agent
        While ( $\tau < \max_{iter}$ )            $\forall$  serch agent
Update B, Q, u, z and s
    If ( $s < 0.5$ )           // pre-processing
        Update the present search agent location as per LU-WOA Eq. (25)
    Else if ( $|B| \geq 1$ )           // Localization
        Update the present search agent location as per Eq. (24)
    Else if ( $S \geq 0.5$ )           // segmentation
        Update the present search agent location as per Eq. (21)
    End if
Update  $A_i$ 
End while
Return  $A_i$ 
    
```

**Stop**

*Output: finest solution*

---

### 4.3 Objective Function

The main objective of this paper is to improve the accuracy of IVD localization and segmentation. For this purpose, the proficiency of WOA is employed and updated using Lagrangian concepts. Eq. (27) defines the fitness function  $F$  of LU-WOA and the objective of this paper, where  $i$  the number of iteration is and  $j$  is the input image

given for optimization.

$$FF = \max(\text{Accuracy})_i^j \quad (27)$$

#### 4.4 Solution Encoding

Since U-Net is a unique NN architecture, it exposes FCN computational characteristics. Even though U-Net provides significant performance, there is always a space for the betterment with respect to precise outcomes in the field of image processing. Intending to attain improvised accuracy for IVD segmentation, the weight parameter of the final convolution layer of U-Net is optimized using the LU-WOA model. Specifically, the contraction path performs down-sampling which encodes the input features and eliminates insignificant features. Thereby, it reduces the feature space and substantially trains the network. Here, the weight parameter in the down-conv4 layer is optimized with the constant  $c$  to attain considerable performance, where  $c = 0.5$ . Fig. 4 depicts the graphical representation of optimization of U-Net using the LU-WOA Model. Moreover, Fig. 5 portrays the solution encoding of LU-WOA, where  $W$  is the weight parameter of U-Net.

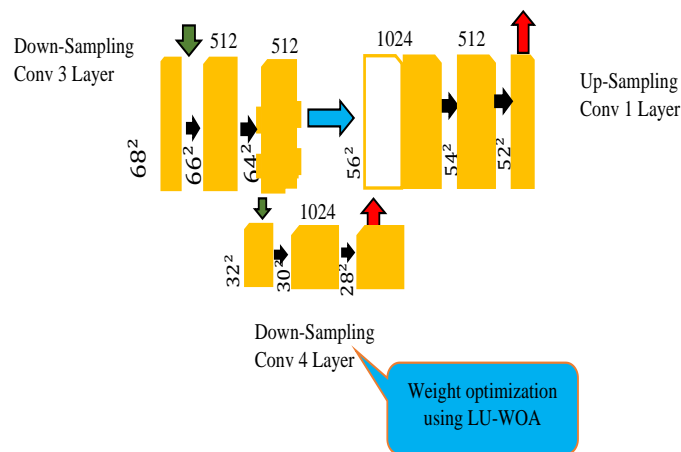


**Fig.4 Graphical Representation of Optimization of U-Net using LU-WOA Model**

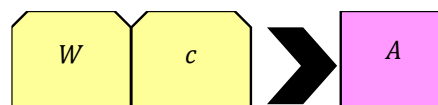


**Fig.5 Solution Encoding of Proposed LU-WOA Model**

Here, the proposed U-Net based LU-WOA Model model was utilized to analyse the affected part of the Intervertebral Disc. Consequently, the collected images are preprocessed and localized. After the localization, easy to analyse the affected part because localized images are identify the two or more features in an image. Moreover, this technique is not only applicable for this domain. It is applicable for various domain like object detection fields, facial recognition etc.

#### 5. Simulation Results

The proposed Image Segmentation model using the ML approach was implemented in MATLAB 2018a on Intel core® core i3 processor 7020U@2.3 GHz, 8 GB RAM, 64-

bit operating system. Here, a multi-modal MRI Dataset was employed for localizing and segmenting IVD which is available in the link IVDM3Seg - Overview (weebly.com)[Access date: 11-10-2021].The efficiency and novelty of the implemented model were recorded via the simulation results. Here, the evaluation was implemented through various performance parameters such as accuracy, sensitivity, specificity, and DSC using multi-modal MRI data. Furthermore, the performance of the proposed model is compared over various conventional models like DCNN [32], SVM [8], NN [4], SOTA [37] and FCN [5].

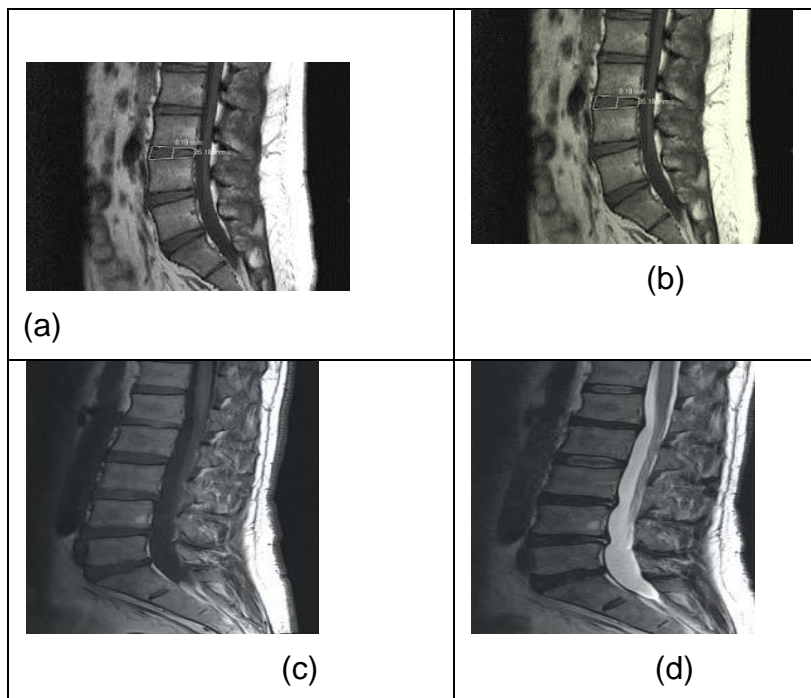
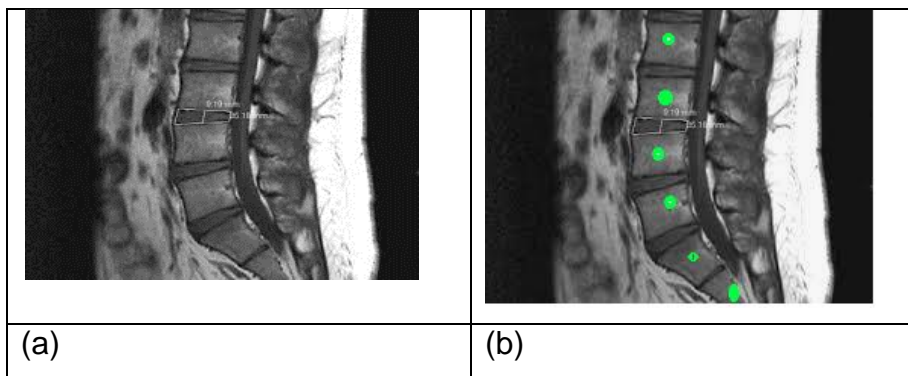
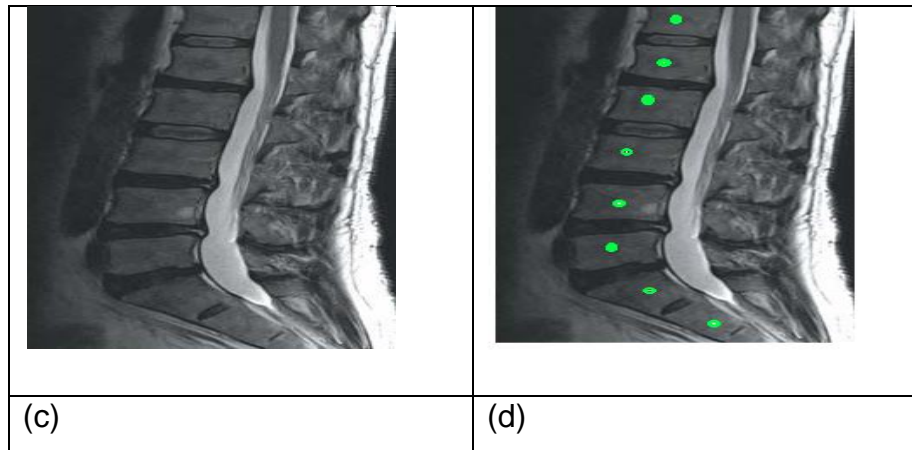


Fig.6 Sample Images Showing Original Image (a) and (c), and Filtered Images (b) and (d)





**Fig.7 Sample Images Depicting Localization of Spines using Edge Detection and Centroid Estimation**

### 5.1 Performance Analysis

The proposed IVD localization and segmentation model using the LU-WOA-UNet algorithm is addressed here. Fig. 6 shows the samples of original images  $I_{input}$  and filtered images  $G_{out}$ . Furthermore, Fig.7. Portrays the sample images depicting localization of spines using edge detection and centroid estimation. These images are further given to segmentation using the proposed LU-WOA-UNet model. The segmentation process carried out by the UNet segmentation model is given in Fig. 8. Here, these are the image results attained after performing the basic operations of the proposed LU-WOA-UNET algorithm. From the investigation, it is evident that the proposed model exposed better performance and accuracy as far as precise localization and segmentation of IVDs

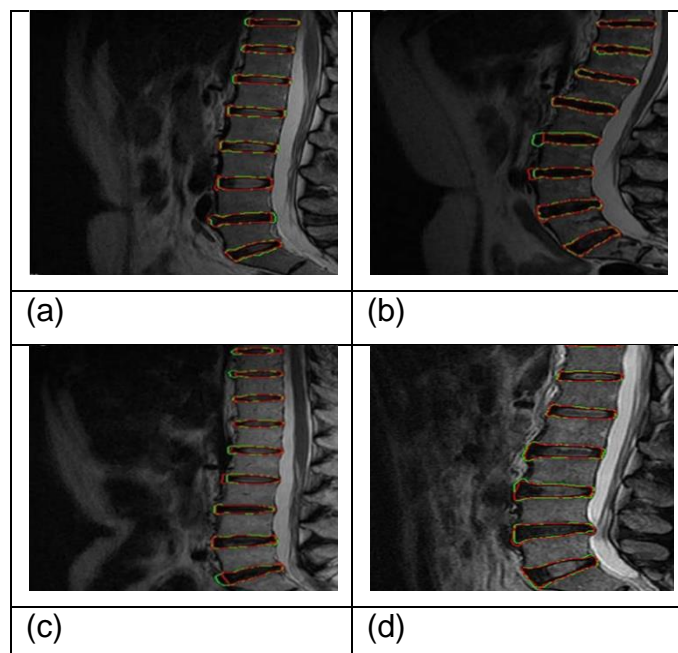


**Fig.8 Sample Images portraying UNet Segmentation Model of iVD MRI**

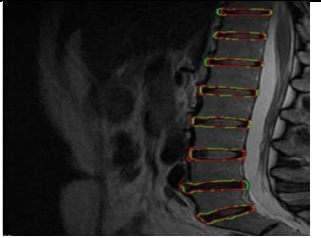
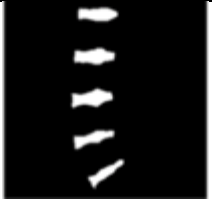
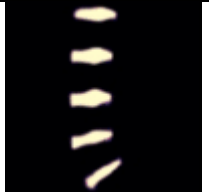
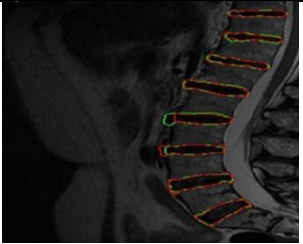
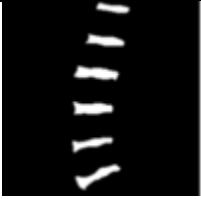
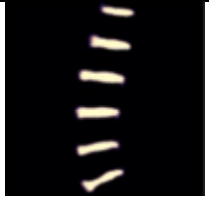
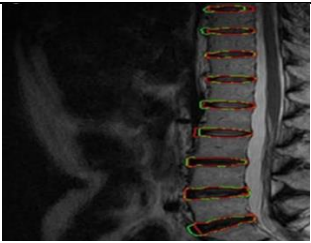
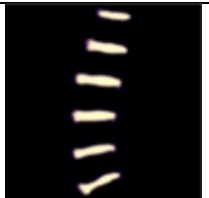
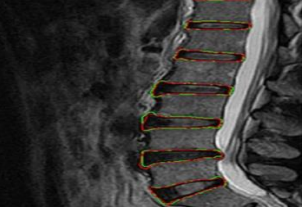
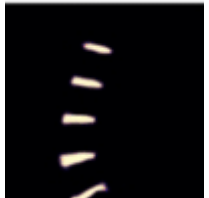
- **Segmentation**

Here the affected parts are segmented with the support of proposed optimization fitness function. Primarily, affected parts of the images are masked using the U-Net based LU-WOA model. Moreover, the mask U-Net based LU-WOA model is compared with traditional RCNN replica. For the implementation, 70% of data has been taken as the training process and 30 of data has been taken as testing process. Here, the training process the WOA parameters are initiated to the U-Net model structures and convergence are validated with other models. The training time of the learning rate is reasonable and accurate prediction for all datasets. The U-Net model has 4 convolution blocks and increase the feature size.

## 5.2 Comparative Analysis

The comparative analysis of the proposed IVD localization and segmentation model using the LU-WOA-UNet algorithm is presented here. The performance of the proposed LU-WOA-UNet algorithm is evaluated using the metrics viz accuracy, sensitivity, specificity, and DSC. Fig. 9 shows the experimental results of the LU-WOA-UNet algorithm. Herein, Fig. 9(a) depicts the convergence graph of performance metrics like accuracy, sensitivity, specificity, and DSC are illustrated. Moreover, the UNet is trained with 50% of data and tested with 50% of data throughout the entire optimization process. At the 40th iteration, the accuracy is around 80 and at the 100th iteration, the optimal accuracy of 96.45% is attained. On the other hand, Fig. 9(b) portrays the localization of IVDs using various conventional models such as NN, FCN, SVM, and DCNN and the Proposed LU-WOA-UNet. At this point, the illustration is given for 10 images showing a number of localized IVDs. For image 4, the proposed model localized around 9 IVDs whereas NN localized 7, FCN localized 6, SVM localized 7, and DCNN localized 8. From this investigation, it is clear that the proposed LU-WOA-UNet accomplished enhanced performance than the other models. Moreover, Fig. 10 showing the bar plot demonstrating a comparison of performance metrics in terms of accuracy, sensitivity, specificity, and DSC. In Fig. 10(a), the performance of the “with and without optimization” model is depicted. The accuracy of the proposed LU-WOA-UNet algorithm attained enhanced performance which is 8.12%, and 2.65% improved than only UNet and conventional WOA-UNet models respectively. Similarly, in Fig. 10(b) the proposed model accomplished 8.76%, 5.07%, 5.01, and 3.47% better than NN, FCN, SVM, and DCNN respectively. In addition, Fig. 11 portrays the results attained from varying the training percentage. Particularly, Fig. 11(a) illustrating a comparative evaluation of the proposed LU-WOA-UNet algorithm in terms of accuracy which is 7.02% better than NN, 4.44% better than FCN, 5.1% improved than SVM, and 3.62% better than DCNN for 70% of training data. Besides, the proposed LU-WOA-UNet algorithm achieved considerable sensitivity which is 6.42%, 4.89%, 5.3%, and 3.15% improved than NN, FCN, SVM, and DCNN respectively for 80% of training data. On considering specificity, the proposed LU-WOA-UNet algorithm gained 6.14%, 4.12%, 5.1%, and 2.98% better than NN, FCN, SVM, and DCNN respectively for 30 % of training data. At last, for DSC estimation of 50% of training data, the proposed LU-WOA-UNet algorithm achieved 6.91% better than NN, 3.98% better than FCN, 5.3% improved than SVM, and 3.14% better than DCNN. From the empirical study, it is evident that the proposed LU-WOA-UNet algorithm attained better results and outperformed the conventional models.

**Table.II Comparison of standared segmented mask image**

Original image	U-Net segmented image	Segmented mask image (proposed)	Segmented mask image (existing RCNN)
			
			
			
			

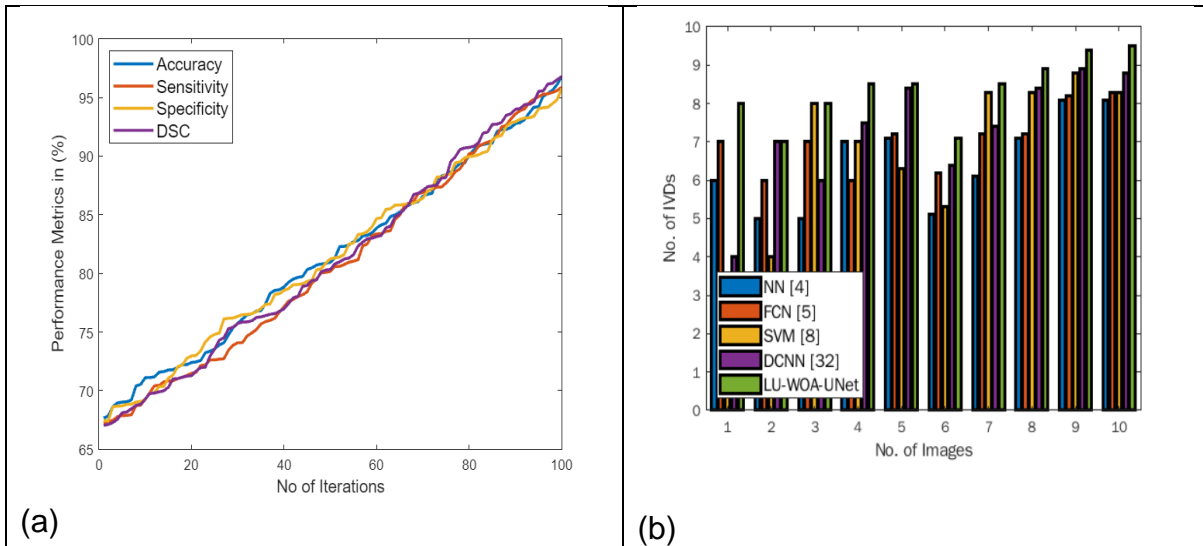


**Fig.9 Investigation Study showing (a) Convergence of Accuracy, Sensitivity, Specificity, and DSC, and (b) Localization of IVDs using various Conventional Models and the Proposed LU-WOA-UNet**

Table II shows the overall performance of the proposed LU-WOA-UNet model and the other conventional models in terms of DSC. It summarizes the mean, median, min, and max values of the DSC score attained by proposed and conventional models. Here, the mean value of the proposed LU-WOA-UNet model is higher than the other traditional models which are 7.29%, 5.49%, 4.17%, and 1.3% better than NN, FCN, SVM, and DCNN respectively. For median values, the proposed LU-WOA-UNet model accomplished 0.7924 of DSC which is 8.5% better than NN, 5.88% improved than FCN, 3.45% better than SVM, and 2.25% better than DCNN. For maximum values, the proposed LU-WOA-UNet model obtained 0.9678 of DSC which is 8.26% better than NN, 4.88% improved than FCN, 4.04% better than SVM, and 3.06% better than DCNN. Eventually, for minimum values, the proposed model gains 11.5%, 7.78%, 5.7%, and 3.89% better than NN, FCN, SVM, and DCNN respectively. Thereby, the proposed LU-WOA-UNet algorithm efficiently performs localization and segmentation of IVDs and proved its competence by outperforming the conventional models.

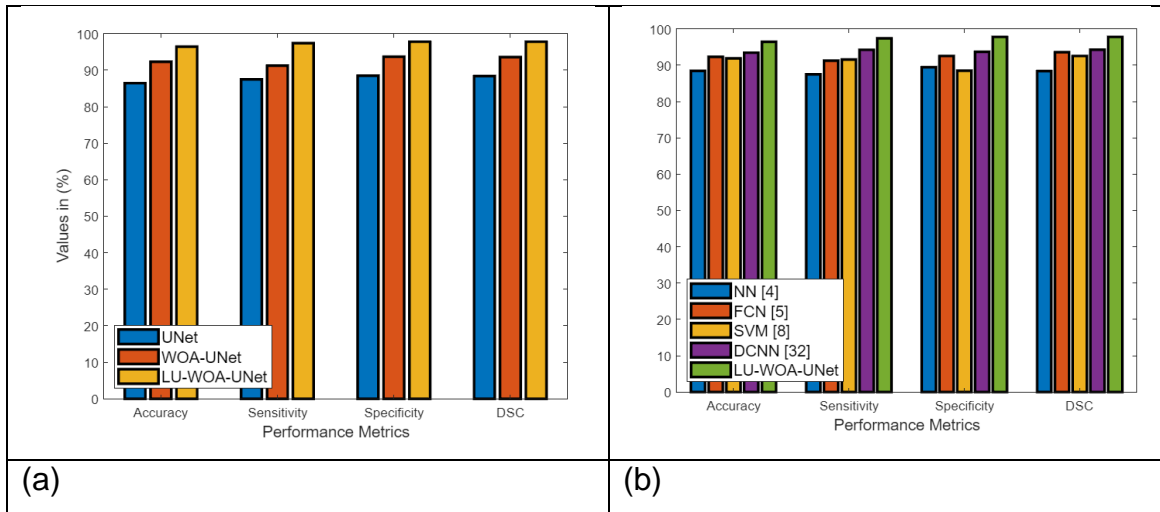


**Fig.10** Bar Plot demonstrating a comparison of performance metrics in terms of Accuracy, Sensitivity, Specificity, and DSC (a) for only UNet model, WOA-UNet and Proposed LU-WOA-UNetModel, and (b) other Conventional Models and Proposed LU-WOA-UNetModel

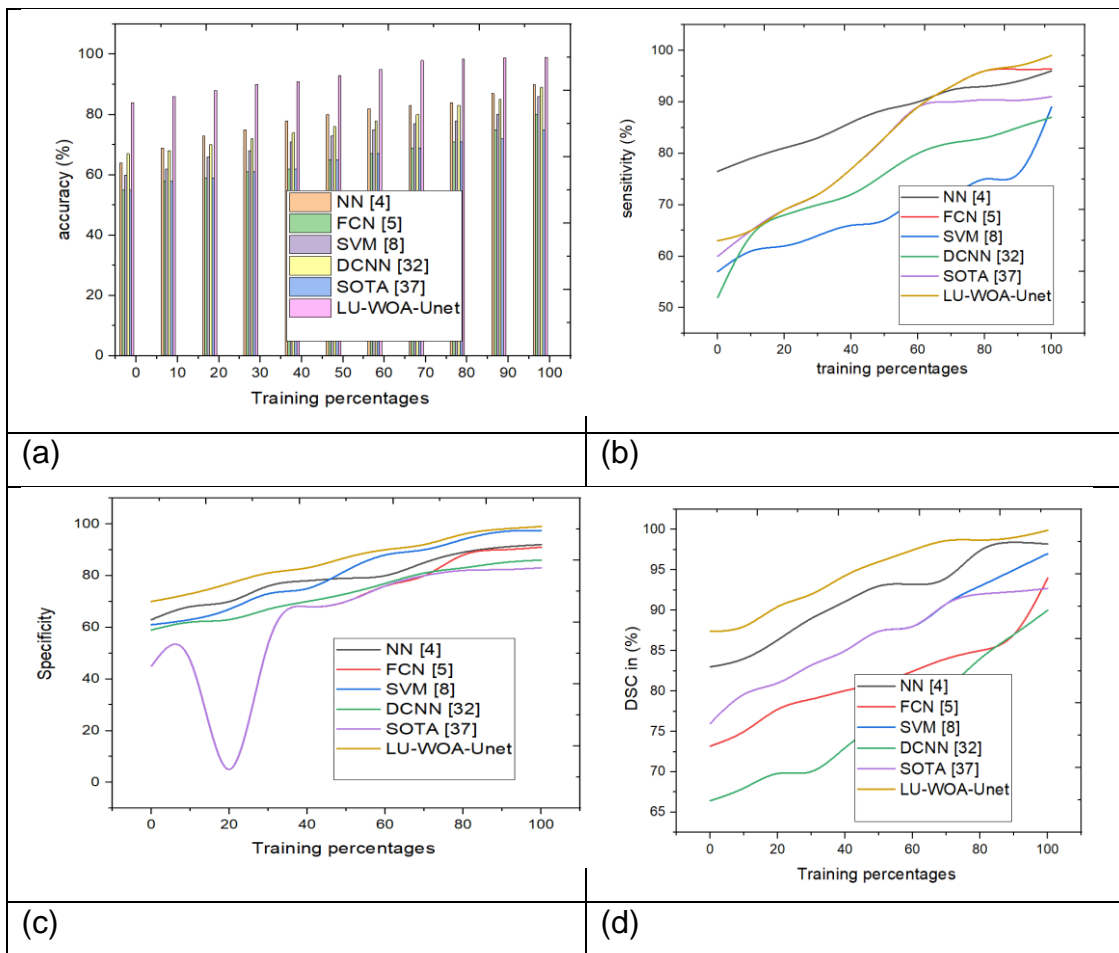


**Fig.11** Comparative Evaluation Showing Results on Varying the Training Percentage of Proposed LU-WOA Model and other Trational Models by means of (a) Accuracy, (b) Sensitivity, (c) Specificity, and (d) DSC

**TABLE II Overall Segmentation Results of Proposed LU-WOA-UNet Algorithm and other Conventional Models concerning DSC**

Metrics	NN [4]	FCN [5]	SVM [8]	DCNN [32]	SOTA [37]	Proposed LU-WOA-UNET
Mean DSC	0.4561 ± 0.023	0.465 ± 0.0123	0.4715 ± 0.133	0.486 ± 0.145	0.4474 ± 0.027	0.492 ± 0.012
Median	0.725	0.7458	0.7651	0.7745	0.7811	0.7924
Max	0.8878	0.9214	0.9287	0.9381	0.952	0.9678
Min	0.6821	0.711	0.727	0.741	0.753	0.771

## 6 Conclusion

This paper has introduced a novel IVD localization and segmentation model using the efficiency of U-Net. Initially, multi-modal MRI data were taken as input images for IVD localization. Now, the noises in the input images were eliminated through a data pre-processing phase using the Gaussian filtering technique. After removing unnecessary data in the input images, the filtered images were subjected to localization, and the localized images are given to the U-Net model for segmentation. Eventually, the image segmentation was carried out using U-Net which was optimized via the competence of LU-WOA. Also, the significance of the proposed model was verified and validated through a comparative analysis over the traditional models such as DCNN, SVM, NN, and FCN methods. The performance of the “with and without optimization” model was presented and the accuracy of the proposed LU-WOA-Unet algorithm attained enhanced performance which was 8.12%, and 2.65% improved than only UNet and conventional WOA-UNet models respectively. Similarly, the proposed model accomplished 8.76%, 5.07%, 5.01, and 3.47% better than NN, FCN, SVM, and DCNN respectively. In this way, the competence and efficiency of the proposed LU-WOA-UNet model were proved and validated. In the future, data from multiple datasets containing MRI, CT, and X-rays will be implemented for IVD localization and segmentation.

## References

- 1) Das P, Pal C, Acharyya A, Chakrabarti A, Basu S, “Deep neural network for automated simultaneous intervertebral disc (IVDs) identification and segmentation of multi-modal MR images”, *Comput Methods Programs Biomed*, Vol. 205, Apr 2021.
- 2) S. Kim W. Bae K. Masuda C. Chung and D. Hwang "Fine-grain segmentation of the intervertebral discs from MR spine images using deep convolutional neural networks: BSU-Net" *Applied Sciences* vol. 8 no. 9 pp. 1656 2018.
- 3) Yang Y, Wang J, Xu C, “Intervertebral Disc Segmentation and Diagnostic Application Based on Wavelet Denoising and AAM Model in Human Spine Image”, *J Med Syst*, Vol. 6, 2019.
- 4) Abhinav Suri, Brandon C. Jones, Grace Ng, Nancy Anabaraonye, Patrick Beyrer, Albi Domi, Grace Choi, Sisi Tang, Ashley Terry, Thomas Lechner, Iman Fathali, Nikita Bastin, Helene Chesnais, and Chamith S. Rajapakse, "A deep learning system for automated, multi-modality 2D segmentation of vertebral bodies and intervertebral discs", *Bone*, Vol. 149, August 2021.

- 5) Li X, Dou Q, Chen H, Fu CW, Qi X, Belavý DL, Armbrecht G, Felsenberg D, Zheng G, Heng PA, "3D multi-scale FCN with random modality voxel dropout learning for Intervertebral Disc Localization and Segmentation from Multi-modality MR Images", *Med Image Anal*, Vol. 45, pp. 41-54, Apr2018.
- 6) Wimmer M, Major D, Novikov AA, and Bühler K, "Fully automatic cross-modality localization and labeling of vertebral bodies and intervertebral discs in 3D spinal images", *Int J Comput Assist Radiol Surg*, Vol. 13, No. 10, pp. 1591-1603, Oct 2018.
- 7) Belavy DL, Owen PJ, Armbrecht G, Bansmann M, Zange J, Ling Y, Pohle-Fröhlich R, and Felsenberg D, "Quantitative assessment of the lumbar intervertebral disc via T2 shows excellent long-term reliability", *PLoS One*, Vol. 16, No. 4, Apr 2021.
- 8) Hashia, B., and Mir, A.H, "Texture features' based classification of MR images of normal and herniated intervertebral discs", *Multimed Tools Appl*, Vol. 79, pp. 15171–15190, 2020.
- 9) Zheng G, Chu C, Belavý DL, Ibragimov B, Korez R, Vrtovec T, Hutt H, Everson R, Meakin J, Andrade IL, Glocker B, Chen H, Dou Q, Heng PA, Wang C, Forsberg D, Neubert A, Fripp J, Urschler M, Stern D, Wimmer M, Novikov AA, Cheng H, Armbrecht G, Felsenberg D, Li S, "Evaluation and comparison of 3D intervertebral disc localization and segmentation methods for 3D T2 MR data: A grand challenge", *Med Image Anal*, Vol. 35, pp. 327-344, Aug 2017.
- 10) Zhu X, He X, Wang P, He Q, Gao D, Cheng J, Wu B, "A method of localization and segmentation of intervertebral discs in spine MRI based on Gabor filter bank", *Biomed Eng Online*, Vol. 22, pp. 15:32, Mar 2016.
- 11) Chen C, Belavy D, Yu W, Chu C, Armbrecht G, Bansmann M, Felsenberg D, Zheng G, "Localization and Segmentation of 3D Intervertebral Discs in MR Images by Data Driven Estimation", *IEEE Trans Med Imaging*, Vol. 34, No. 8, pp. 1719-1729, Aug 2015.
- 12) C. Wang, Y. Guo, W. Chen and Z. Yu, "Fully Automatic Intervertebral Disc Segmentation Using Multimodal 3D U-Net," 2019 IEEE 43rd Annual Computer Software and Applications Conference (COMPSAC), pp. 730-739, 2019.
- 13) C. Chen D. Belavy and G. Zheng "3D intervertebral disc localization and segmentation from MR images by data-driven regression and classification" *International Workshop on Machine Learning in Medical Imaging* pp. 50-58 2014.
- 14) H. Chen Q. Dou X. Wang and P. A. Heng "Deepseg: Deep segmentation network for intervertebral disc localization and segmentation" *Proc. 3rd MICCAI Workshop & Challenge on Computational Methods and Clinical Applications for Spine Imaging* 2015.
- 15) Dolz, José, Christian Desrosiers and Ismail Ben Ayed, "IVD-Net: Intervertebral disc localization and segmentation in MRI with a multi-modal UNet.", *ArXiv abs/1811.08305*, (2018).
- 16) M. Urschler K. Hammernik T. Ebner and D. Štern "Automatic intervertebral disc localization and segmentation in 3d mr images based on regression forests and active contours" *International Workshop on Computational Methods and Clinical Applications for Spine Imaging* pp. 130-140 2015
- 17) I. Lopez and B. Glocker "Complementary classification forests with graph-cut refinement for ivd localization and segmentation" *Proc. the 3rd MICCAI Workshop & Challenge on Computational Methods and Clinical Applications for Spine Imaging* 2015.
- 18) W. Mbarki, M. Bouchouicha, S. Frizzi, F. Tshibas, L. Ben Farhat and M. Sayadi, "A novel method based on deep learning for herniated lumbar disc segmentation," 2020 4th International Conference on Advanced Systems and Emergent Technologies (IC\_ASET), pp. 394-399, 2020.
- 19) Isaac Castro-Mateos Rui Hua Jose M Pozo Aron Lazary and Alejandro F Frangi "Intervertebral disc classification by its degree of degeneration from t2-weighted magnetic resonance images" *European Spine Journal* vol. 25 no. 9 pp. 2721-2727 2016.
- 20) R. Korez B. Ibragimov B. Likar F. Pernuš and T. Vrtovec "Deformable model-based segmentation of intervertebral discs from MR spine images by using the SSC descriptor" *International Workshop on Computational Methods and Clinical Applications for Spine Imaging* pp. 117-124 2015.

- 21) J. T. Lu S. Pedemonte B. Bizzo S. Doyle K. P. Andriole M. H. Michalski et al. "DeepSPINE: Automated Lumbar Vertebral Segmentation Disc-level Designation and Spinal Stenosis Grading Using Deep Learning" arXiv preprint arXiv:1807.10215 2018.
- 22) H. Chen Q. Dou X. Wang J. Qin J. CY Cheng and P. A. Heng "3D fully convolutional networks for intervertebral disc localization and segmentation" International Conference on Medical Imaging and Virtual Reality pp. 375-382 2016.
- 23) A Neubert J Fripp C Engstrom D Walker MA Weber R Schwarz et al. "Three-dimensional morphological and signal intensity features for detection of intervertebral disc degeneration from magnetic resonance images" Journal of the American Medical Informatics Association vol. 20 no. 6 pp. 1082-1090 2013.
- 24) M. K. Zeybel and Y. S. Akgül, "Identification and Localization of Lumbar Intervertebral Discs on MRI Images with Faster RCNN," 2019 4th International Conference on Computer Science and Engineering (UBMK), pp. 129-133,2019.
- 25) F. Fallah, S. S. Walter, F. Bamberg and B. Yang, "Simultaneous Volumetric Segmentation of Vertebral Bodies and Intervertebral Discs on Fat-Water MR Images," IEEE Journal of Biomedical and Health Informatics, vol. 23, no. 4, pp. 1692-1701, July 2019.
- 26) M. W. Law K. Tay A. Leung G. J. Garvin and S. Li "Intervertebral disc segmentation in MR images using anisotropic oriented flux" Med. Image Anal. vol. 17 no. 1 pp. 43-61 2013.
- 27) X. Ji G. Zheng L. Liu and D. Ni "Fully automatic localization and segmentation of intervertebral disc from 3D multi-modality MR images by regression forest and CNN" Proc. Int. Workshop Comput. Methods Clin. Appl. Spine Imag. pp. 92-101 2016.
- 28) F. Zhao, K. Dang and H. Liu, "Intervertebral Discs Localization and Segmentation Based on Broad Learning System and IPU-Net," 2021 3rd International Conference on Natural Language Processing (ICNLP), pp. 248-254, 2021.
- 29) H. Q. Liu A. Q. Pi and V. Chaudhary "Broad learning-based intervertebral discs localization and segmentation" Proceedings of the Third International Symposium on Image Computing and Digital Medicine pp. 263-268 2019.
- 30) Iriondo C, Padoia V, and Majumdar S, "Lumbar intervertebral disc characterization through quantitative MRI analysis: An automatic voxel-based relaxometry approach", Magn Reson Med, Vol. 84, No. 3, pp. 1376-1390, Sep 2020.
- 31) Heinrich, Mattias, and Oktay, Ozan, "Accurate Intervertebral Disc Localisation and Segmentation in MRI Using Vantage Point Hough Forests and Multi-atlas Fusion", Conference: International Workshop on Computational Methods and Clinical Applications for Spine Imaging pp. 77-84,2016.
- 32) Jie Fang, QingBiao Zhou, Shuxia Wang, "Segmentation Technology of Nucleus Image Based on U-Net Network", Scientific Programming, vol. 2021, Article ID 1892497, 10 pages, 2021.
- 33) Seyedali Mirjalili, and Andrew Lewis, "The Whale Optimization Algorithm", Advances in Engineering Software, Vol. 95, pp. 51-67, May 2016.
- 34) Jane Jiang, and Paul J.Scott, "Free-form surface filtering using wavelets and multiscale decomposition", Advanced Metrology, pp. 195-246, 2020.
- 35) Iqbal N, Mumtaz R, Shafi U, Zaidi SMH, "Gray level co-occurrence matrix (GLCM) texture based crop classification using low altitude remote sensing platforms", PeerJ Computer Science, Vol. 7, 2021.
- 36) R. M. Haralick, K. Shanmugam and I. Dinstein, "Textural Features for Image Classification," IEEE Transactions on Systems, Man, and Cybernetics, vol. SMC-3, no. 6, pp. 610-621, Nov. 1973.